

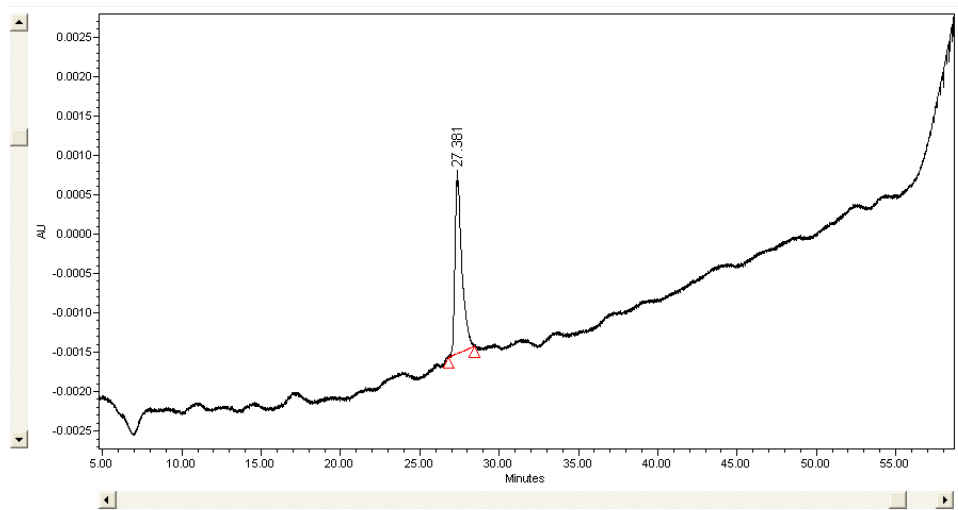
# Engineering the assembly of heme cofactors in man-made proteins

AUTHOR NAMES: Lee. A. Solomon, Goutham Kodali, Christopher C. Moser and P. Leslie Dutton\*

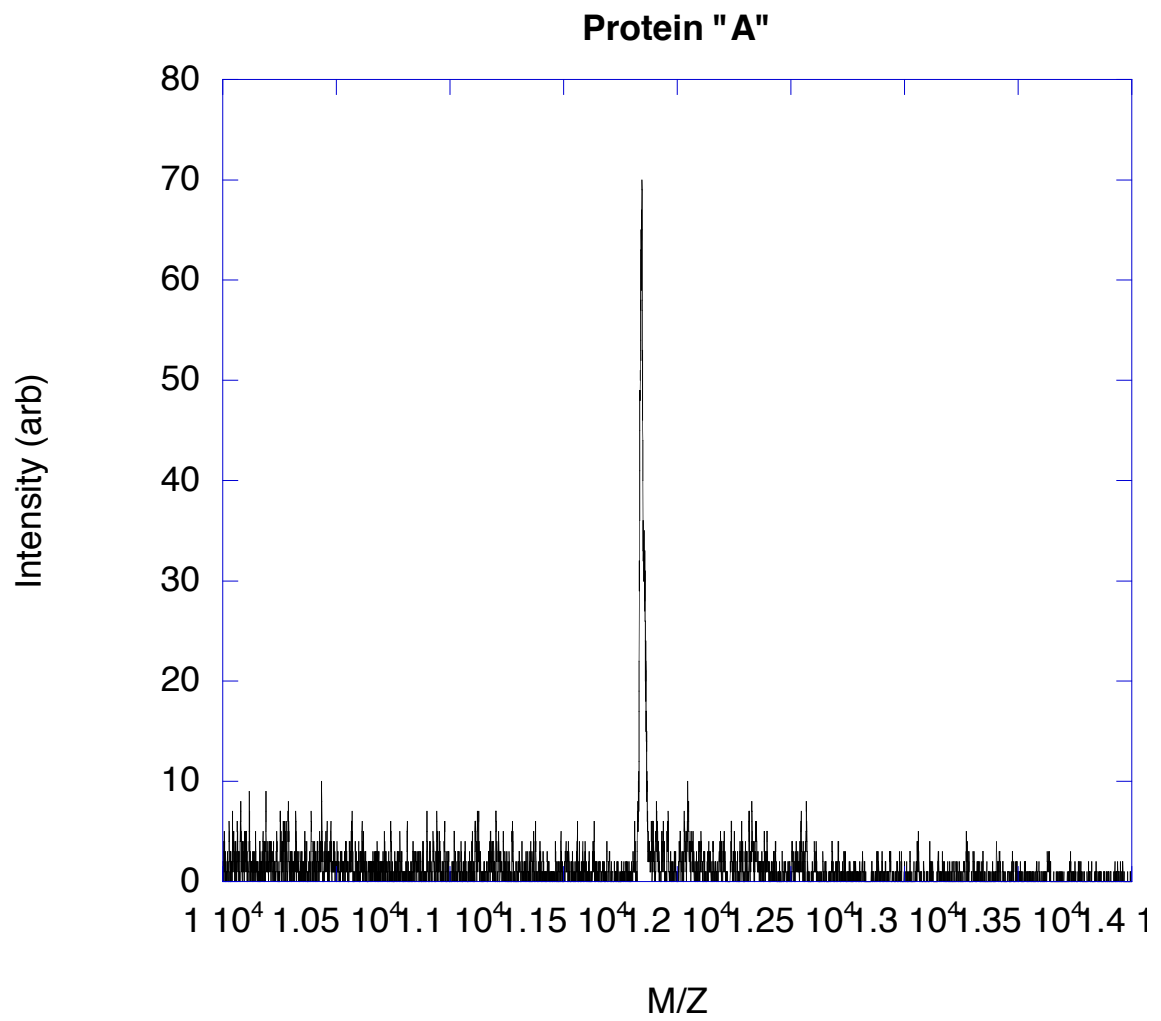
AUTHOR ADDRESS

The Johnson Research Foundation, Department of Biochemistry and Biophysics, University of Pennsylvania, Philadelphia, PA 19104

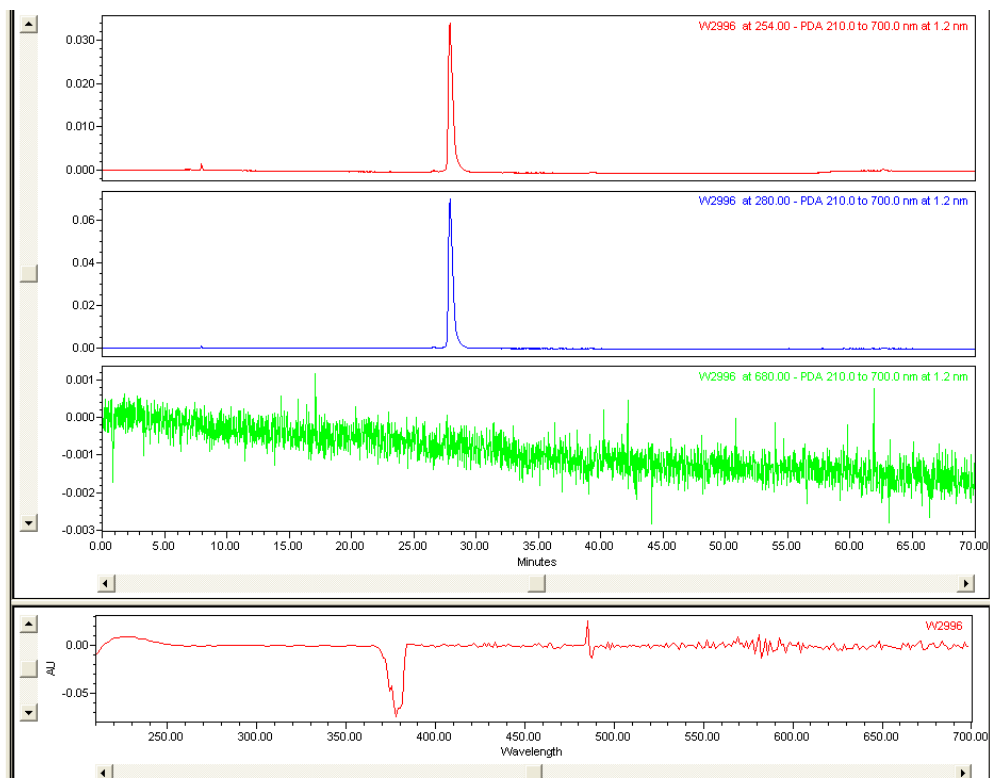
## Supplementary Figures and Tables



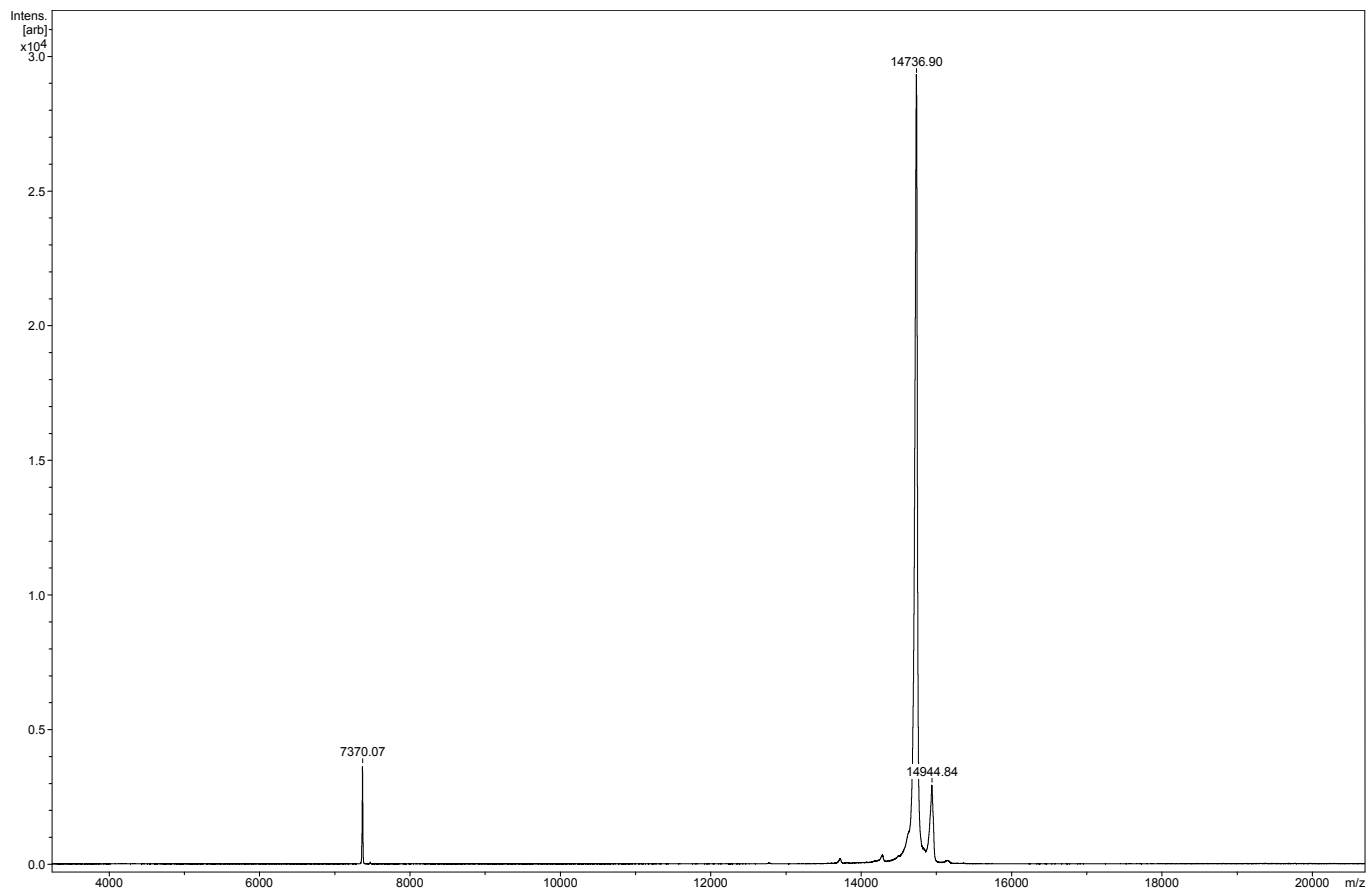
Supplemental Figure 1: HPLC trace of protein A



Supplemental Figure 2: MALDI of Protein A

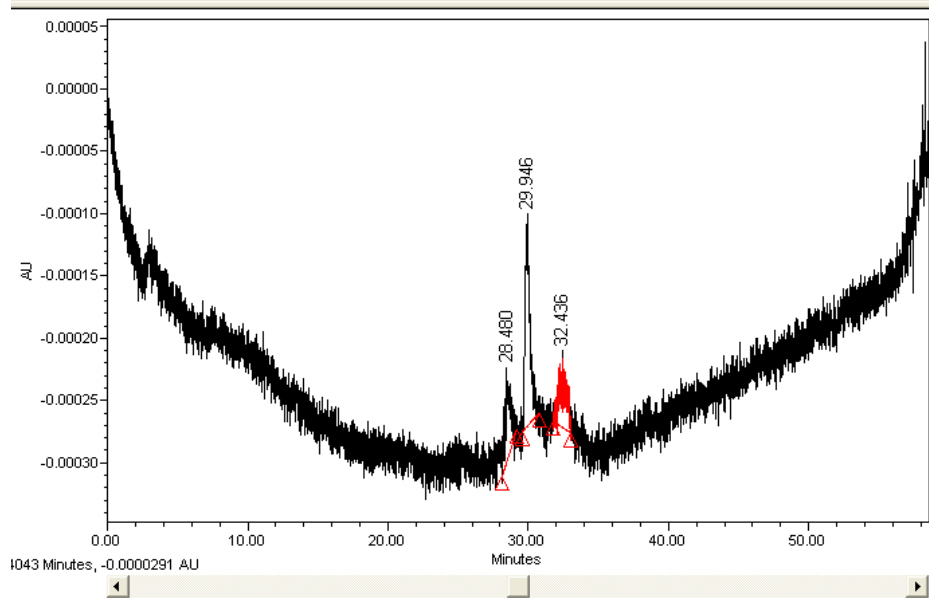


Supplemental Figure 3: HPLC of Protein B

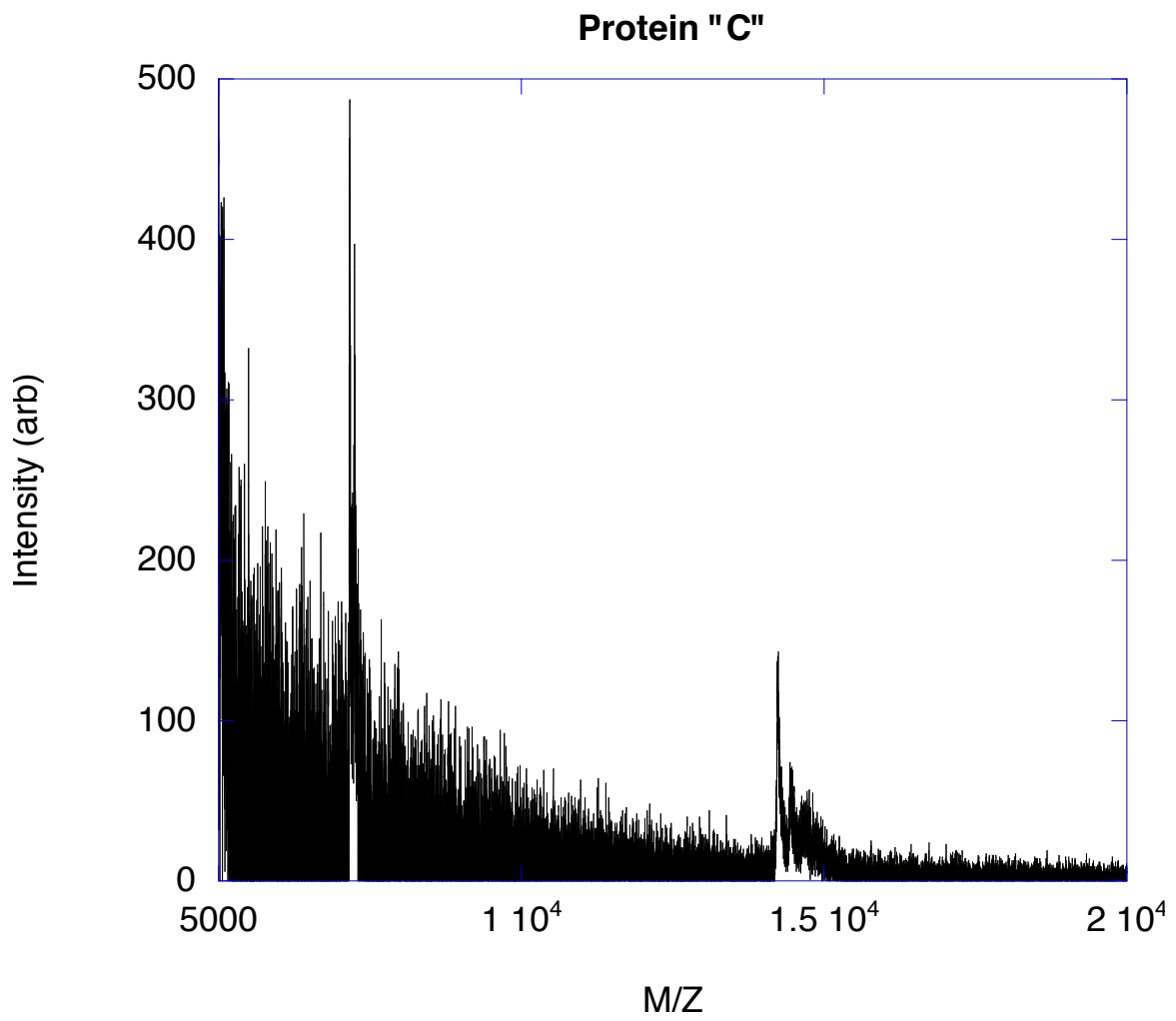


Supplemental Figure 4: MALDI of Protein B

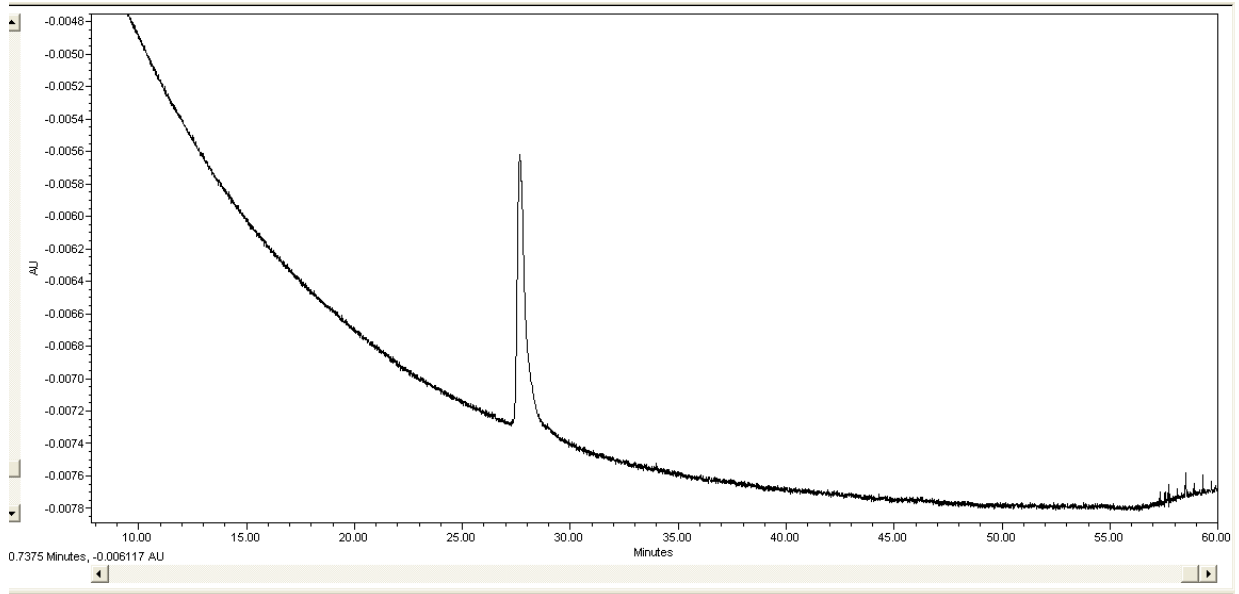




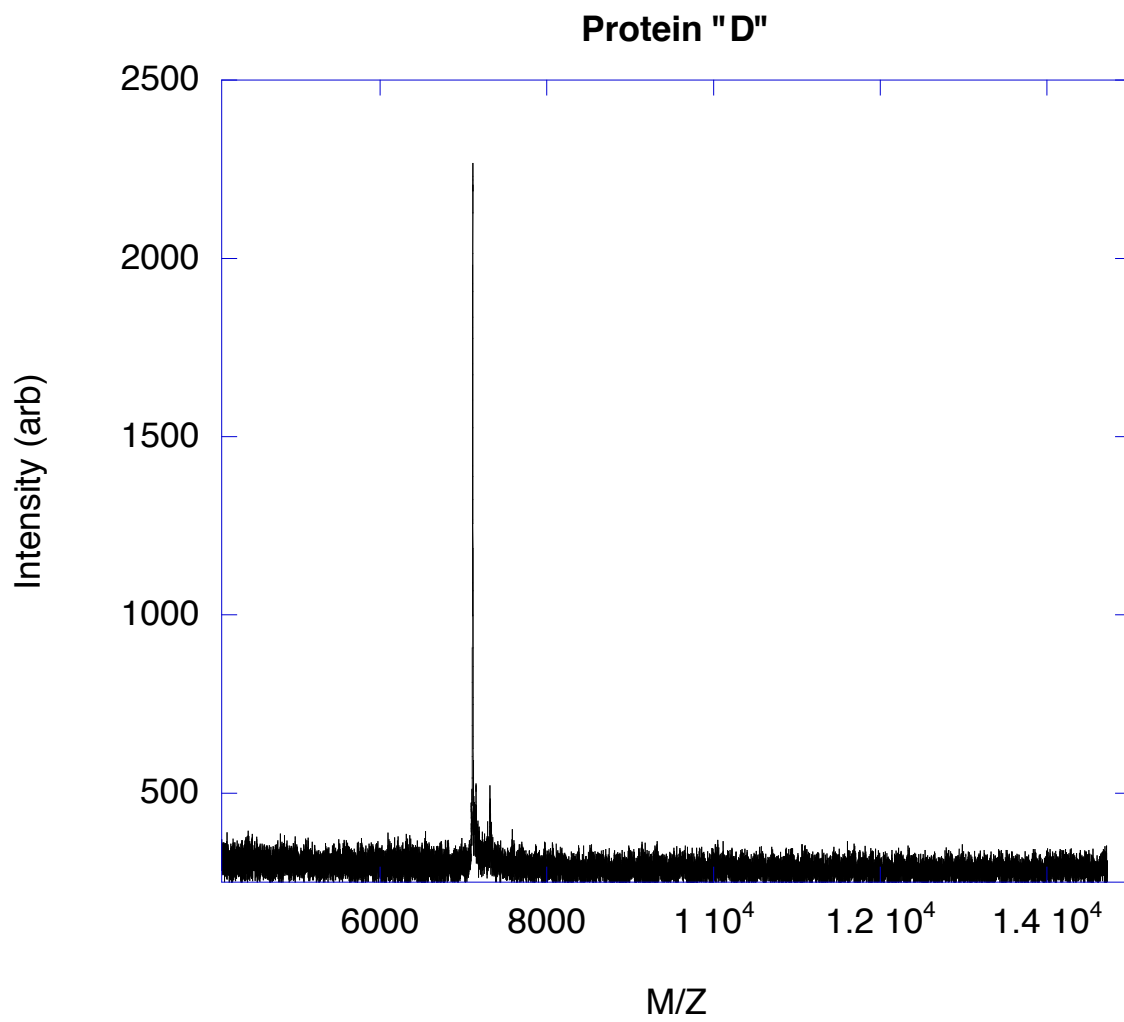
Supplemental Figure 5: HPLC of Protein C. The peak at 28 minutes is the monomer, while the peak at 29 minutes is the dimer.



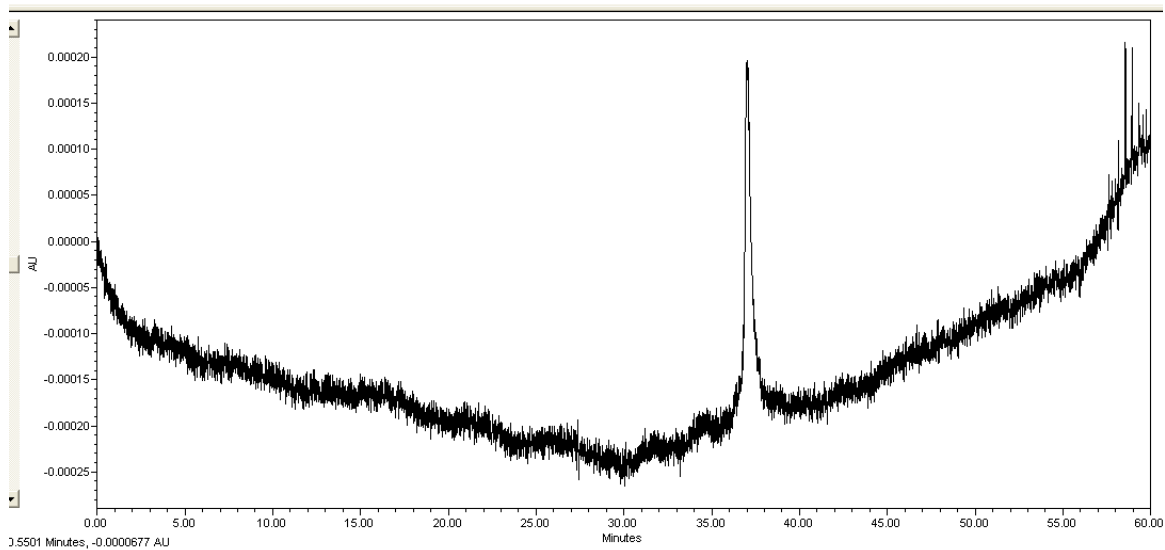
Supplemental Figure 6: MALDI of Protein C



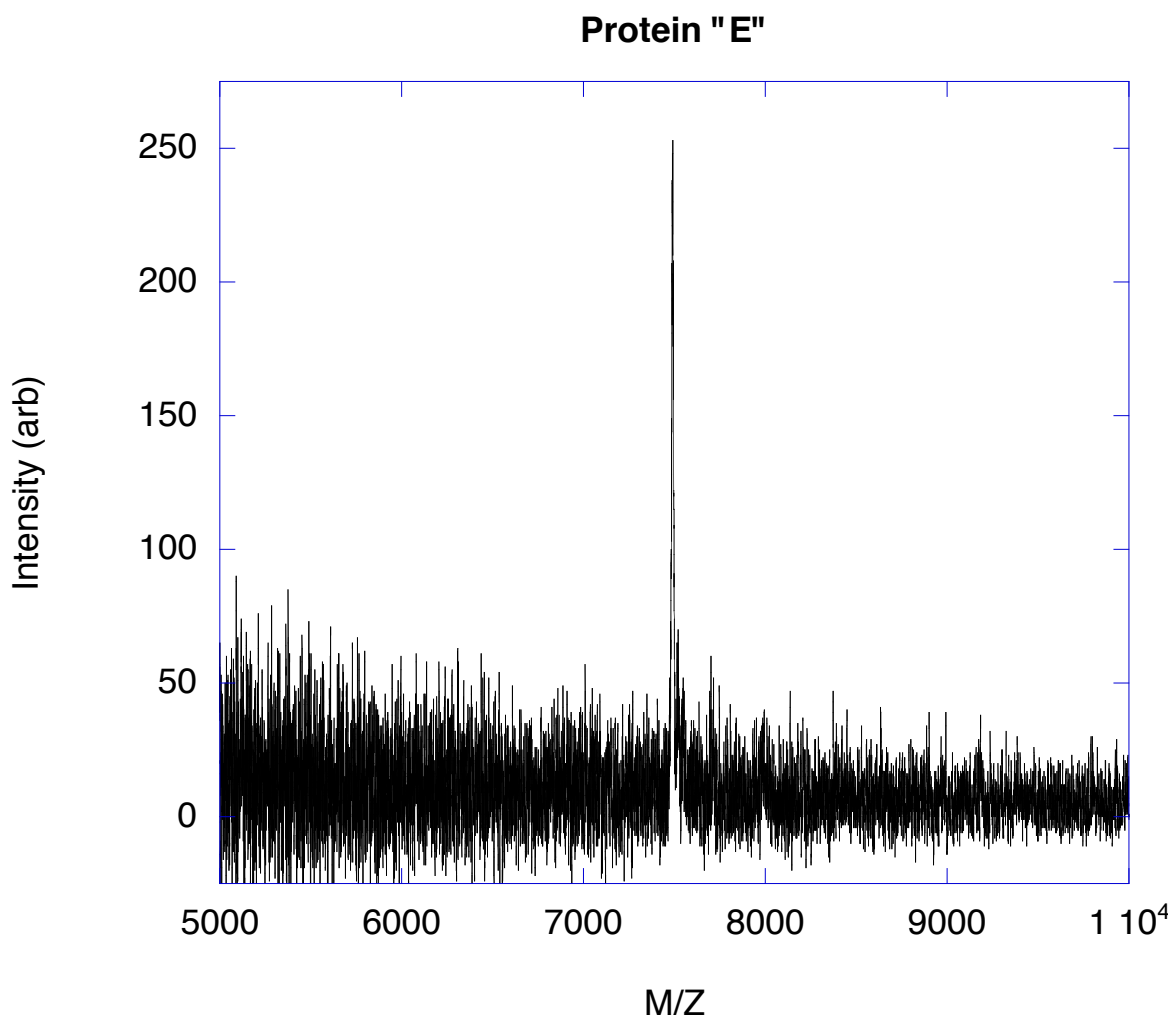
Supplemental Figure 7: HPLC of Protein D



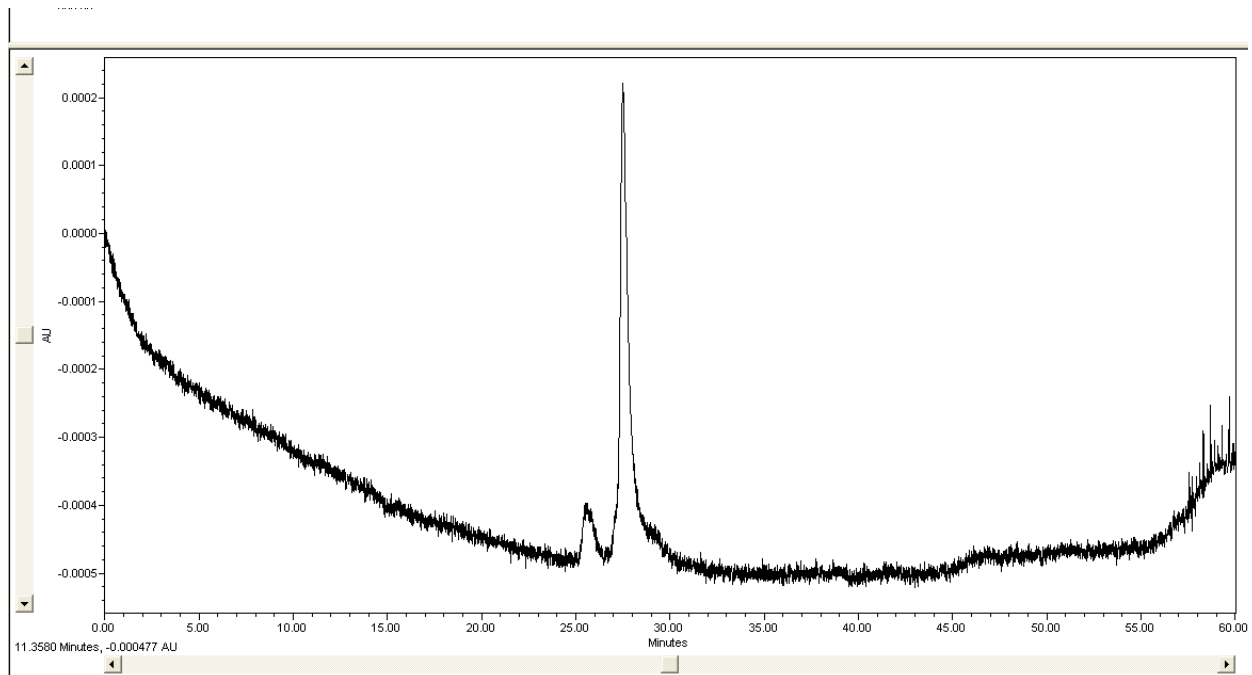
Supplemental Figure 8: MALDI of Protein D



Supplemental Figure 9: HPLC of Protein E

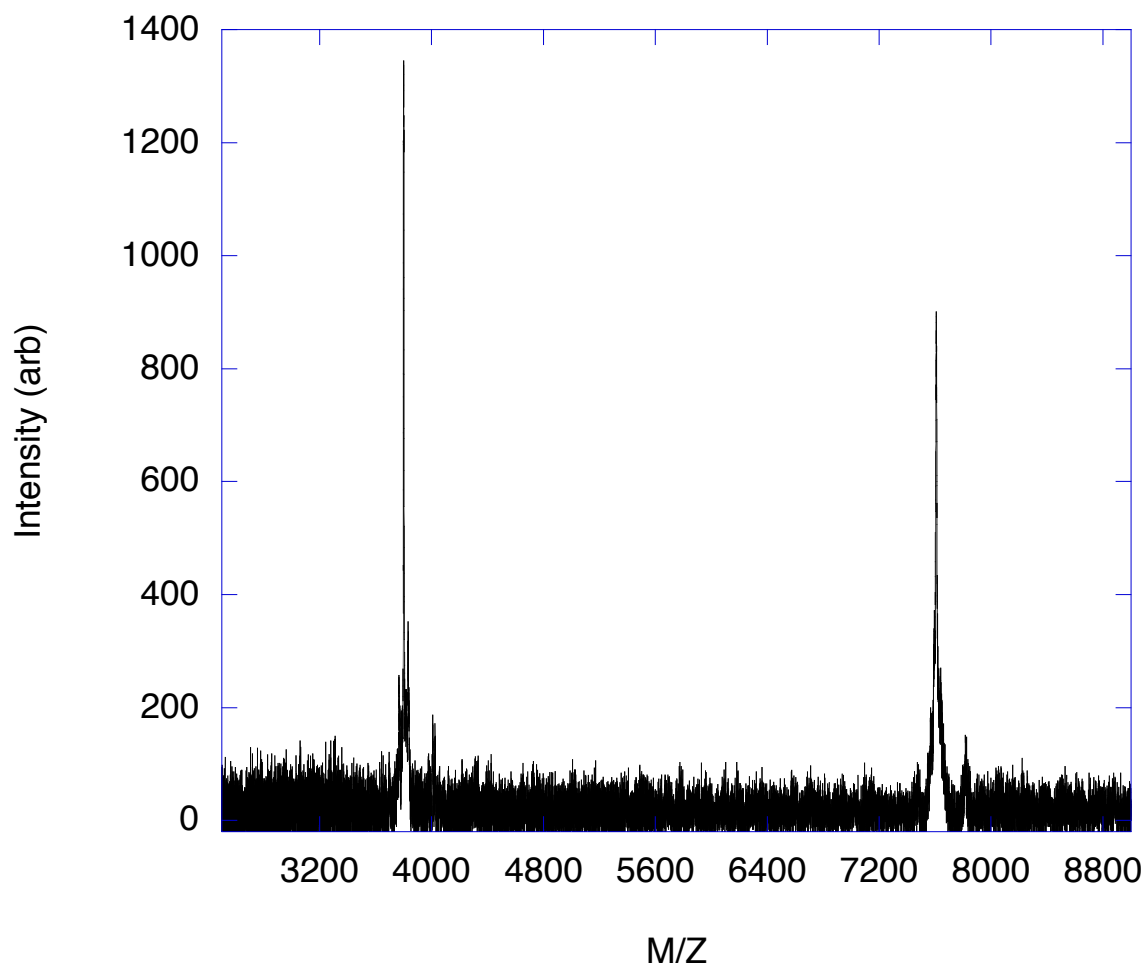


Supplemental Figure 10: MALDI of Protein E in dimer form



Supplemental Figure 11: HPLC of Protein F. The peak at 26 minutes corresponds to the monomer, while the peak at 28 minutes corresponds to the dimer.

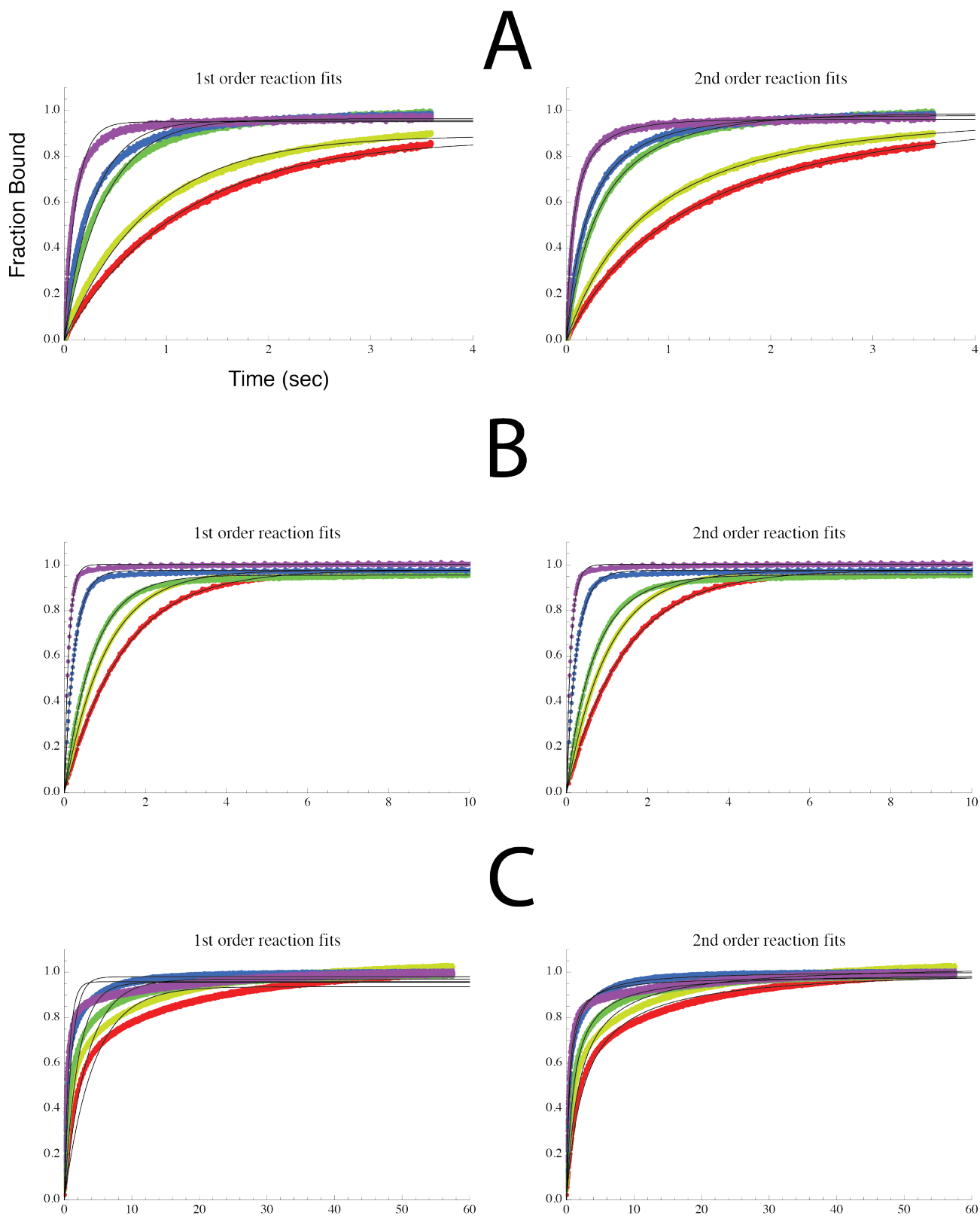
### Protein "F"



Supplemental Figure 12: MALDI of Protein F

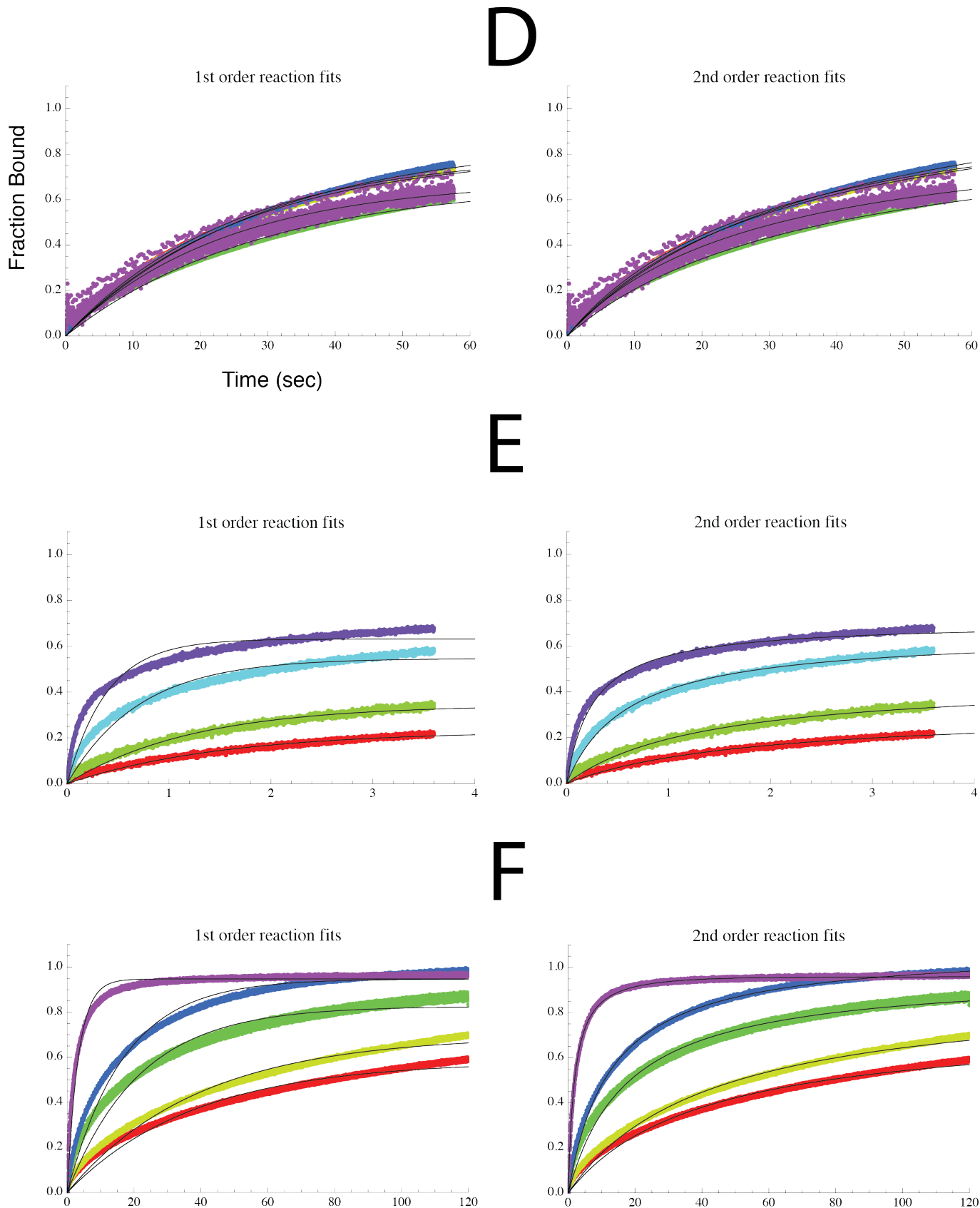
Supplementary Table 1: primary sequence differences within **B – F** maquettes)

Protein	Sequence	Reference
A	ADLEDNMETLNDNLKVIKADNAAQVKDALTKMRAAALDAQKATPPKLEDKSPDPEMKDF RHGFDILVGGQIDDALKLANEGKVKEAQAQAAAEQLKTTRNAYHQKYR	(15)
B	GEIWKQHEDALQKFEDALNQFEDLKQLGGSGSGSGG EIWKQHEDALQKFEDALNQFEDLKQLGGSGSGSGG EIWKQHEDALQKFEDALNQFEDLKQLGGSGSGSGG EIWKQHEDALQKFEDALNQFEDLKQL	(1)
C	GEIWKQHEDALQKFEDALNQFEDLKQLGGSGCGSGG EIWKQHEDALQKFEDALNQFEDLKQL	(12)
D	GEIWKQHEDALQKFEDALNQFEDLKQLGGSGSGSGG EIWKQHEDALQKFEDALNQFEDLKQL	--
E	CGGGELWKLHEELLKKFEELLKLAERLKKL	(11)
F	CGGGEIWKLHEEFLLKKFEELLKLHEERLKKM	(39)

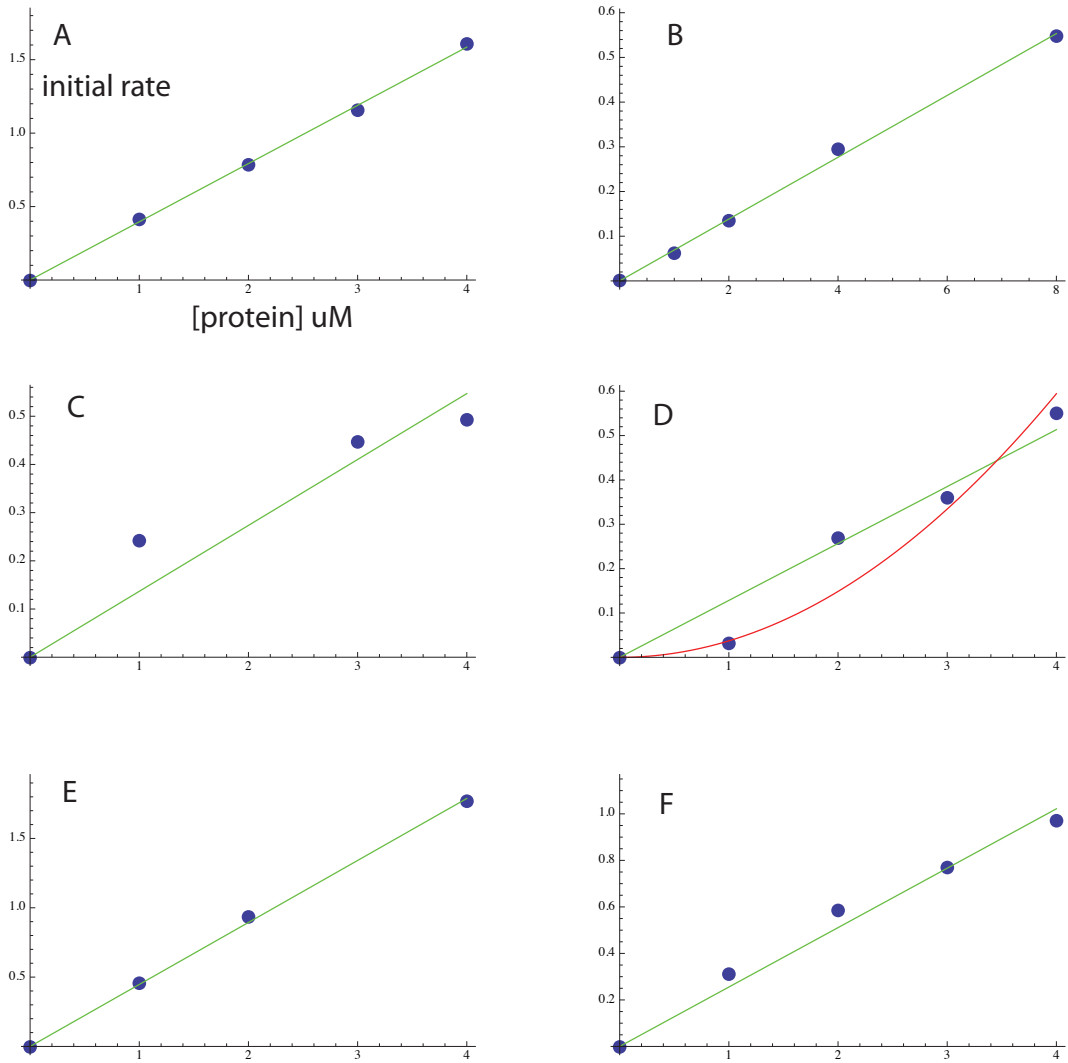


Supplementary Figure 13: Heme binding kinetics for maquette **A** **B** and **C** at various temperatures fit to either a first order (left) or a second order (right) time course. Heme and total number of bis-His binding sites equimolar at 10  $\mu$ M. Temperatures are as follows: Purple: 45°C, Blue: 30°C, Green: (**A**: 25°C, **B**: 21°C, **C**: 22°C), Yellow: 15°C, and Red: 10°C.

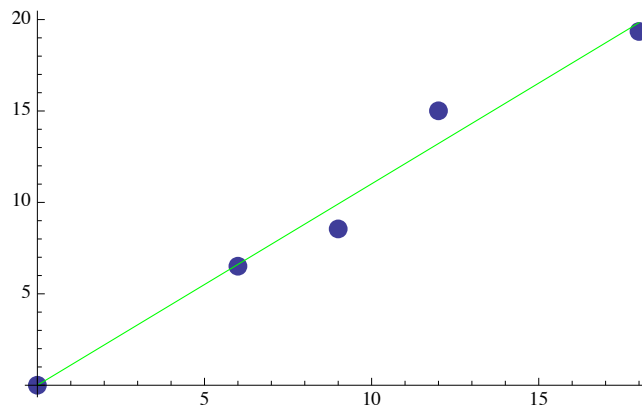




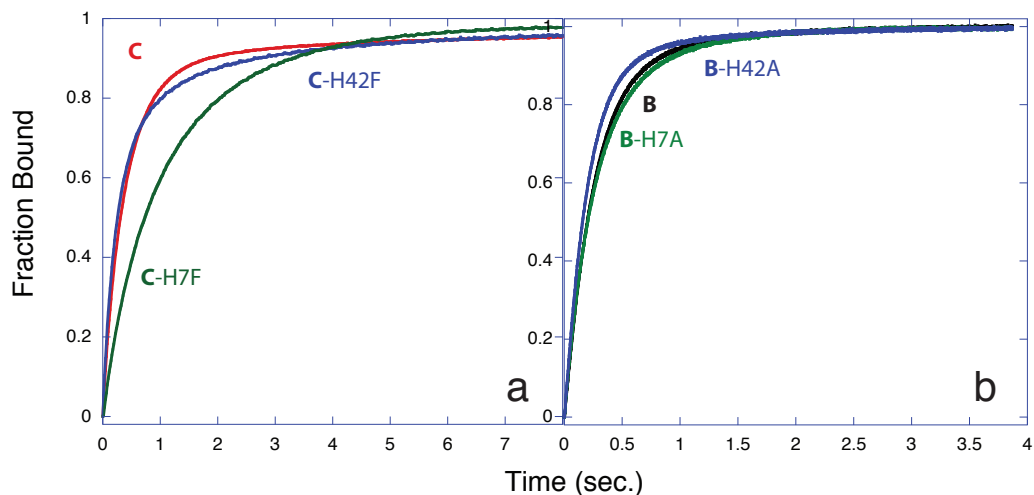
Supplementary Figure 14: Heme binding kinetics for maquette **D E** and **F** at various temperatures fit to either a first order (left) or a second order (right) time course. Heme and total number of bis-His binding sites equimolar at 10  $\mu$ M. Temperatures are as follows: Purple: 45°C, Blue: 30°C, Green: (**D**: 20°C, **F**: 25), Yellow: 15°C, and Red: 10°C.



Supplementary Figure 15: initial rate of heme binding as a function of protein concentration for sequences **A** through **F**. Sequence **D**, showing the initial rate of the slow non-burst phase, can be fit equally well to a linear or quadratic dependence on the protein concentration.



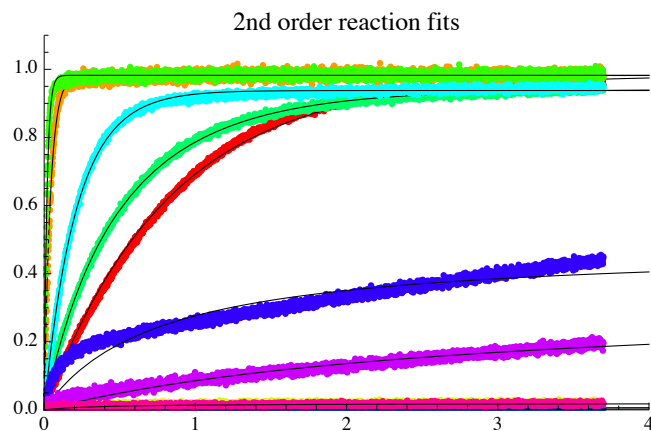
Supplementary Figure 16: initial rate of heme binding as a function of heme concentration to protein **B**.



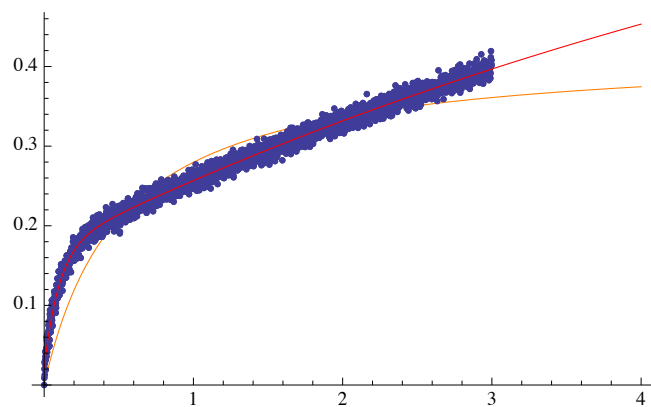
Supplemental Figure 17: Rates for (A) maquette **C** and its site knockout mutants. The H42F and wild-type variants share similar rates, but the H7F variant binds heme much slower. This is due to differences between the two sites.<sup>13</sup> (B) Maquette **B** and its individual site knockouts. Unlike **C**, all variants of **B** share the same kinetics with halftimes within 40 msec of one another. All data was collected at 20°C in 20mM CHES 150mM KCl buffer pH 9.

Porphyrin	Rate constant ( $M^{-1} s^{-1}$ )	Log-P (CHES pH 9)	$K_D$ Values (nM)
Hemin	82068	0.46254	<2
Mesoporphyrin	484079	0.55195	<10
Deuteroporphyrin	176639	0.65704	80
IsoHematoporphyrin	58649	0.1196	1120
DADPIX	30371	0.12379	<10
Etioporphyrin	3796	1.4218	--
FePPIX-DME	3140	0.85306	--
Tetracarboxyphenyl porphyrin	12557	0.02769	--
2,6-Dinitrile porphyrin	7118	0.036413	--
Heme a	683	0.93846	--

Supplemental Table 2: Rate and affinity data for the porphyrins used in this work. Due to the slow binding rate of Etioporphyrin, Tetracarboxyphenyl porphyrin, Fe-Protoporphyrin IX Dimethyl Ester, 2,6-Dinitrile porphyrin and Heme A  $K_D$  values were unable to be obtained. The presence of side reactions such as aggregation, and the lack of data describing the kinetic and thermodynamic parameters of them, hinders our ability to calculate valid numbers.



Supplemental Figure 18: Second order fits for the porphyrin binding reactions. Mesoporphyrin: Green, Deuteroporphyrin: Orange, Heme: Teal, IsoHematoporphyrin: Turquoise, Diacetyl Deuteroporphyrin: Red, Tetracarboxyphenylporphyrin: Blue, 2,6-Dicyanoporphyrin: Purple, Protoporphyrin IX Dimethyl Ester: Pink, Etioporphyrin: Yellow, and Heme  $\alpha$ : Blue.



Supplemental figure 19: Fe-Tetracarboxyphenylporphyrin assembly kinetics fit to a biphasic (Red), and a second order (orange) reaction equation.